Hyperbranched Molecules with Epoxy-Functionalized Terminal Branches: Grafting to a Solid Surface

A. Sidorenko,[†] X. W. Zhai,[†] F. Simon,[‡] D. Pleul,[‡] and V. V. Tsukruk*,[†]

Materials Science & Engineering Department, Iowa State University, Ames, Iowa 50011, and Institut für Polymerforschung Dresden, Hohe Strasse 6, 01069 Dresden, Germany

Received September 26, 2001

ABSTRACT: We report the fabrication of a molecular surface coating from an epoxy-functionalized hyperbranched polyester functionalized by secondary epoxy groups. These groups were presented in the fraction of terminal branches of the hyperbranched shell with the ratio of epoxy-containing branches and alkyl branches of 1:2. We demonstrated that a uniform monolayer with the thickness of 4.5 nm could be fabricated by melt grafting of functionalized hyperbranched polymers to a bare silicon surface. Steric constraints imposed by the chemical attachment of alkyl and epoxydized branches to a single core prevented microphase separation of dissimilar segments and allowed the fabrication of uniform monolayers with surface exposure of the functional groups and high adhesion. An estimated 3−4 epoxy groups per molecule were located in the uppermost surface layer and provided residual functionality sufficient to graft another polymer layer. Grafted layers were extremely robust and sustain high compression and shear stresses while possessing high elasticity.

Introduction

Fabrication of molecular organic coatings is a powerful tool for controlling interfacial properties of solid substrates and inducing appropriate surface functionality and chemical composition. To ensure temporal stability, direct chemical binding of a surface layer to an underlying substrate is considered to be critical. Three major approaches are widely used for this purpose: grafting macromolecular chains with functional groups from solution or melt with the formation of polymer brush layer (grafting-to approach), growth of a polymer layer by initialization of polymerization process on a functionalized template (grafting-from approach), and the fabrication of self-assembled monolayers (SAMs) by chemisorption from solution.

Surface modification with functionalized SAMs has been shown to be an effective approach, and SAM-based modification is considered to be the benchmark for many technological applications.[1−3] However, despite significant progress in the controlled modification of the chemical surface reactivity, the functional SAMs showed some limitations, such as difficulties in tailoring surface concentration of the functional groups. One-component SAMs possessed a high surface concentration of functional groups with the surface area close to 0.2 nm^2 per group (Scheme 1). The overall surface concentration of functional groups can be changed via "dilution" with an additional component and the fabrication of mixed SAMs. This approach was proven useful for control of surface properties such as wettability, adhesion, and friction within a wide range.[4,5] However, mixing two different components usually resulted in the nonuniform molecular structures caused by the differences in diffusion and reaction rates and, to great rate, to the microphase separation (Scheme 1). Surface morphology of such monolayers was presented by a domain microstructure with lateral sizes of domains on a scale of 10−100 nm. For many nanoscale applications, such a heterogeneous microstructure represented a major challenge for designing controlled nanoscale contacts.[6,7]

Scheme 1. Cartoon of the Microstructural Organization of Organic SAMs and Mixed SAMs with Microphase Separation (top) and a Polymer Brush Layer and a Layer with a Hyperbranched Core and Multifunctional Terminal Branches (bottom)

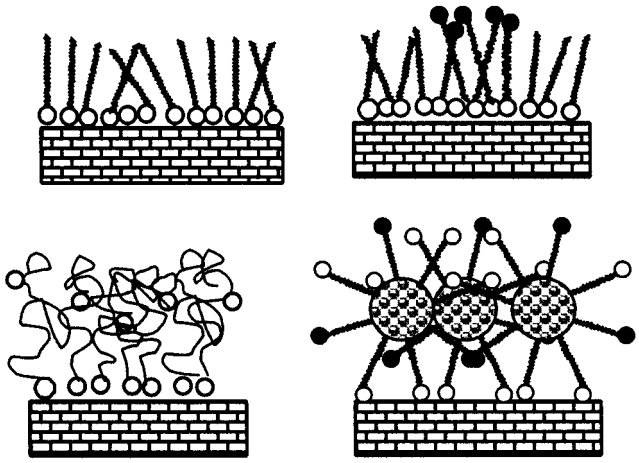

On the other hand, grafting of long-chain macromolecules results in the formation of a robust surface layer with thickness in the range of 1−10 nm as defined by molecular mass of chains and their grafting density.[8] High grafting density ensures a "brush" regime in which macromolecular chains are stretched along the surface normal.[9] It was found that the initial film thickness and the molecular weight of the polymer influence the layer morphology and thickness in a complicated way.[10] A linear decrease in the maximum achievable grafting density with molecular weight was observed. This was explained in part by an entropic barrier that opposes the addition of new chains to the grafted layer. For many of these polymer layers a dewetting morphology was observed for intermediate grafting densities.[11] Moreover, even for uniform polymer brush layers, the

[†] Iowa State University.
[‡] Institut für Polymerforschung Dresden.
* To whom correspondence should be addressed. E-mail vladimir@iastate.edu.

10.1021/ma011682t CCC: $22.00
Published on Web 05/09/2002

distribution of end functional groups is frequently fairly homogeneous which led to screening of buried functional groups (Scheme 1).[12]

In our attempt to overcome these limitations, we turned our attention to functionalized hyperbranched polymers with highly branched, treelike chemical microstructure of macromolecules.[13] These polymers, if grafted properly to a surface, may form uniform layers with a significant fraction of terminal functional groups located at the surface due to space constrains imposed by their treelike architecture.[14] Growing functional hyperbranched layers by the grafting from technique was demonstrated by Crooks et al.[15] He observed fairly uniform layers with controlled chemical composition and thickness. The presence of different types of chemical groups in the terminal branches can be used for tethering to the solid substrate, stabilization of the layer via internal cross-linking, and surface exposure of the appropriate functional groups (Scheme 1). Thus, in our studies, we focus on the utilization of the functionalized hyperbranched macromolecules for building of anchoring interfacial layers: robust, relatively thick (<10 nm), elastic, multicomponent but uniform, firmly grafted to silicon surfaces, and possessing variable and multiple chemical functionalities originating from a single core. The coexistence of different chemical groups in the terminal branches chemically attached to a single core could be critical for the formation of the surface layer with suppressed tendency toward microphase separation of dissimilar multifunctional arms due to chemical constrains imposed by the core-branches microstructure. The variation of chemical functionalities of the different branches can be an effective route to tailoring the surface properties of such layers without having heterogeneous, microphase-separated microstructures.

In this paper, we report first results on the fabrication of an anchoring layer from a hyperbranched polyester (**EHBP**) with 32 peripheral branches including both alkyl and epoxy-functionalized branches. The polymer is based on tetrafunctional ethoxylated penthaerythritol extended with the third generation hyperbranched polyester of dimethylolpropionic acid as described in several publications.[16,17] The hyperbranched core (**G3**) is functionalized by long alkyl chains (mixture of alkyl tails from C_{12} to C_{24}) with secondary epoxy groups embedded in the fraction of branches (see idealized chemical formulas in Figure 1). The ratio of epoxy-containing branches and alkyl branches is approximately 1:2 which gives approximately 11 epoxy groups embedded in the alkyl shell. In the case of grafted **EHBP**, we expected to obtain the effect of hydrophobization of the silicon surface and fabricate a robust, grafted polymer layer, on one hand, and have a fraction of reactive epoxy groups for further surface chemical modification, on the other. Here, we have to emphasis that the chemical formulas presented here reflect highly idealized structure. Actual hyperbranched polymers of this type contain significant fraction of internal defects caused by internal cyclization, irregular branching, and wide molecular weight distribution.[18] However, we consider these structures as a reasonable approximation that is useful in data interpretation. Moreover, XPS results discussed below show chemical composition that is close to one expected for these structures.

Epoxy-containing dendrimers and hyperbranched polymers are, in fact, used for the enhancement of the interfacial strength of polymer composite materials.[19,20] Recent results demonstrated that hyperbranched polymers with epoxy terminal groups showed enhanced adhesion to several polymer and inorganic surfaces and, thus, can act as an effective adhesive additive for enhanced chemical binding at interfaces.[21] On the other hand, hydroxyl-terminated hyperbranched polymers were used as tougheners for epoxy-containing polymers.[16] Curing of epoxy composites mixed with hyperbranched polymers increased toughness of polymeric materials without compromising other mechanical properties. However, these studies focused mainly either on synthetic routines to obtain epoxy-hyperbranched polymers or on processing of the composites and their final thermomechanical properties. The questions of microstructure and morphology of these hyperbranched polymers at interfaces, interfacial distribution of different branches, and stability of grafted layers were not addressed. We will focus on these critical issues by analyzing chemical grafting of epoxy-terminated hyperbranched polymers on a model oxide surface of silicon.

Experimental Section

The substrates were atomically smooth silicon wafers of the {100} orientation with one side polished (Semiconductor Processing, Co.). Silicon wafers were treated in an ultrasonic bath for 10 min followed by a "piranha" solution (30% concentrated hydrogen peroxide, 70% concentrated sulfuric acid, *hazardous solution*!) bath for 1 h. After a "piranha" bath, the samples were rinsed several times with "Nanopure" water (resistivity of 18 MΩ cm) and dried under a stream of dry nitrogen. All sample preparations were performed inside a Cleanroom 100 facility (Contamination Control Products, Supply King, Inc.). Toluene (spectrophotometric grade) was purchased from Aldrich, and tetrahydrofuran (THF, HPLC grade), acetone (Reagent), methyl alcohol (Reagent), and butyl alcohol (Reagent) were purchased from Fisher Scientific Co. and used as received.

The commercially available hydroxyl-functional hyperbranched polyester of the third generation (**G3**) and epoxy-functional hyperbranched polyester of the third generation (**EHBP**) (see idealized chemical structures and molecular models for extended conformations in Figure 1) were obtained from Perstorp Polyols Inc. The original honeylike liquid was purified as follow. The solution of **EHBP** in 1-butanol (1:3) was prepared and poured in 3-fold excess of methanol and shaken intensely for several minutes. The emulsion obtained was allowed to separate overnight in two layers. The bottom layer was taken out and placed in a vacuum at 50 °C for 24 h to remove the alcohols. Grafting on the silicon substrate was carried out from both solution and melt. For the solution grafting, the substrate was kept in a dilute solution for different time periods and rinsed thoroughly following drying before characterization. For the melt grafting, the 10% THF solution was deposited on the substrate by spin-coating to form a films of different thickness ranging from 100 to 300 nm. Spin-coated films were immediately placed in an oven in Ar atmosphere at different temperatures ranging from 60 to 170 °C for different time periods. The residual ungrafted polymer was removed by multiple washing with THF in the ultrasonic bath at 50 °C.

GPC measurements of the polymer samples were conducted in THF solutions using Waters GPC and polystyrene standards. The thickness of grafted layers was measured with a Compel ellipsometer (InOmTech, Inc.). The averaged thickness of the SiO_2 layer was measured prior to the polymer deposition and used during analysis of the ellipsometry data with a double-layer model.[22] The refractive indices were taken from literature data for polyesters and estimated from molar contributions.[23,24] Modified surfaces were also examined by static contact angle measurements (sessile droplet) using a custom-built instrument combining a microscope and a digital

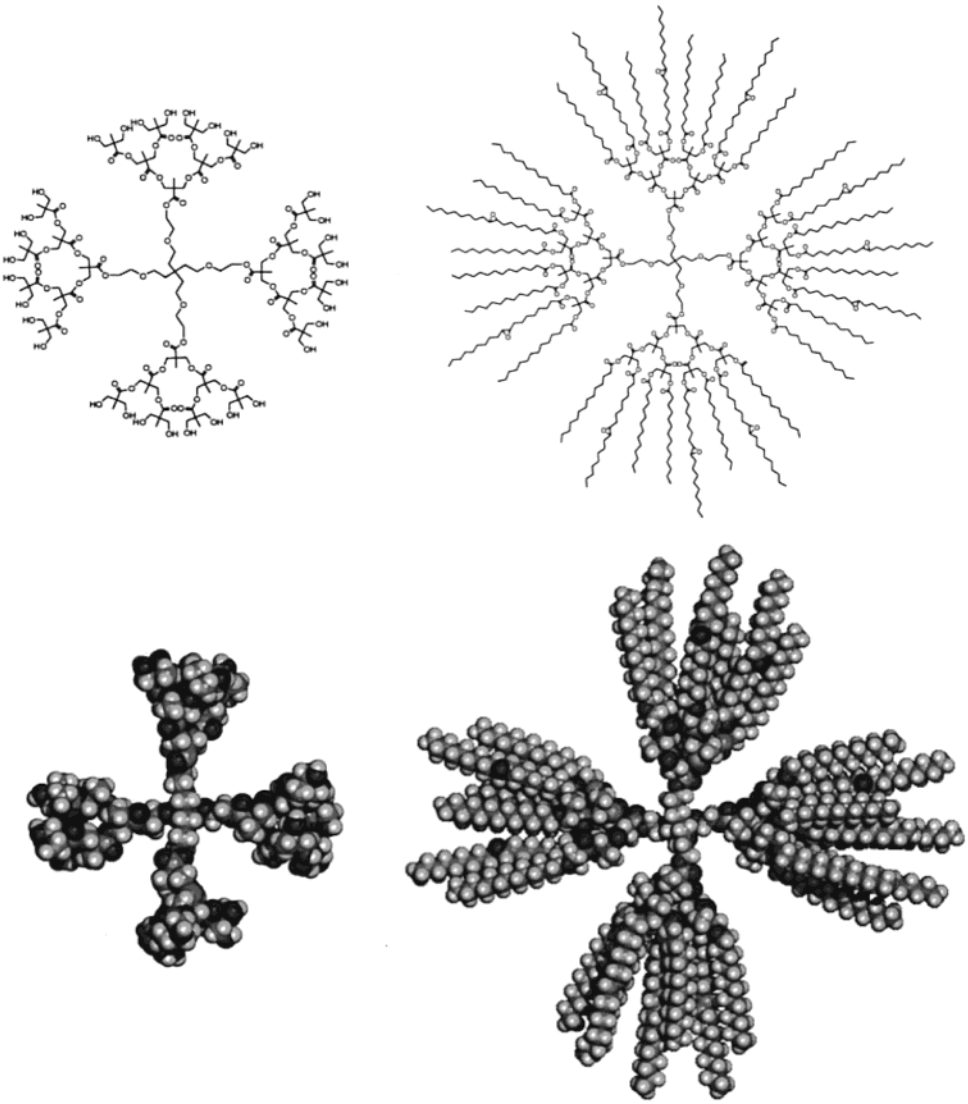

Figure 1. Idealized chemical structures of compounds studied. Top: the hyperbranched polyester core of the third generation (**G3**) (left); the epoxy-containing hyperbranched polyester (**EHBP**) (right). Bottom: the molecular model of corresponding extended conformations. Actual chemical structure contains significant fractions of defects such as internal cyclization, termination, and missing branches. For actual molecules of **EHBP**, fewer than 29 peripheral alkyl chains are presented instead of 32 chains shown for the theoretical model.

camera. Three to five successive measurements were prepared for each sample. ATR-FTIR measurements on a Schimadzu 8300 spectrometer were conducted to confirm chemical composition. The layers were studied with an atomic force microscope (AFM) Dimension-3000 (Digital Instrument, Inc.) in the tapping mode according to an experimental procedure described earlier.[25] To avoid the polymer layer damage, the imaging was performed in the regime of the "light" tapping.[26] The micromapping of surface properties was performed in accordance with the experimental routine reported elsewhere.[27,28] Spring constants of silicon cantilevers of different types were calibrated with the added mass routine, resonant frequency technique,[29] and calibration plots proposed in our previous publications.[30] The tip curvature radii were evaluated by imaging reference samples with tethered gold particles.[31]

AXIS ULTRA (Kratos Analytical) was used for X-ray photoelectron spectroscopy studies. The X-ray-source of Mono-Al $K\alpha_{1,2}$ was operated at 300 W at 20 mA, and a pass energy was selected at 160 eV for survey spectra and 20 eV for high-resolution spectra. To determine the element ratio, normalized peak areas were calculated from initial peak areas (raw area [cps, counts per second]) of the survey spectra according to eq 1, which includes respective sensitivity factors (RSF) and spectrometer's transmission function (tx function):[32]

$$\text{norm area} = \frac{\text{raw area}}{\text{RSF} \times \text{tx function}} \quad (1)$$

To evaluate the chemical composition of the grafted layer, we used the ratio of oxygen and carbon elements obtained experimentally. To separate contributions of the "organic" oxygen from polymer and "silicon" oxygen from dioxide surface layer, we used the following procedure. First, we separated contributions from the "metallic" silicon from bulk and the oxide layer by analyzing the Si 2p spectra taking into account the elemental ratio in the silicon dioxide layer [Si]:[O] as 1:2. The Si 2p spectra were decomposed into three peaks, which corresponded to the two binding states of bulk silicon (Si $2p_{3/2}$ metal and Si $2p_{1/2}$ metal as the result of Russel−Saunders coupling) and Si−O (Si $2p_{3/2}$ = Si $2p_{3/2}$ + $Si_{1/2}$). This separation allowed evaluating the contribution from oxygen associated with the silicon dioxide layer. The residual amount of oxygen was considered related to organic oxygen from the polymer layer.

The molecular volume and dimension calculations were done by a dynamic mechanics execution of the initially fully extended molecular conformation (Figure 1) at an elevated temperature followed by an energy minimization cycle. Simulations were performed on a SGI workstation with Cerius^2 3.9 program.[33] The data were primarily used for the visualization

Table 1. Characteristics of the Hyperbranched Polyesters and Referenced Compounds

	theor M_n[a]	exptl M_n	DPI	contact angle, deg	thickness, nm	theor length/diameter
EHBP	11274	11500	2.6	82	4.5 ± 0.4	3.5−4.5
G3[b]	3604	3400	1.9	42	3.0 ± 0.2	1.5−1.9
OTS SAM[7]	388	NA	NA	110	2.3 ± 0.2	2.5
epoxy SAM[40]	236	NA	NA	52	0.8 ± 0.2	0.9

[a] Calculated for chemical formula presented in Figure 1. [b] Thickness is for the bilayer film.

Scheme 2. Grafting Surface Reaction at Elevated Termperature

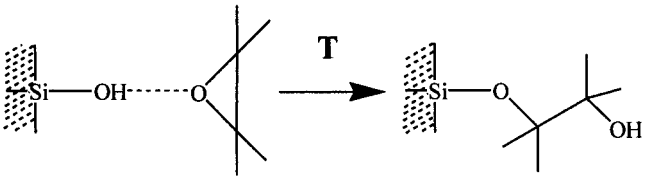

of the molecular shape and the estimation of the most probable molecular dimension. Multiple repetitions of the molecular simulations with different initial conditions showed similar shapes. To build a model with separate packing of a core and terminal branches, we used a polar core in flattened surface conformation built earlier for **G3**,[34] added alkyl branches in predominantly upright positions, and conducted dynamic mechanics runs followed by equilibration to obtain molecular conformation with minimum steric conflicts.

Results and Discussion

GPC analysis of the **G3** and **EHBP** compounds showed molecular weights of 3400 and 11 500 g/mol, respectively (Table 1). A relatively wide molecular weight distribution, as expected, was detected for hyperbranched compounds. Although the GPC results for hyperbranched polymers should be considered with reservations, the experimentally measured molecular weights of both compounds were fairly close to the theoretical value obtained from the idealized models presented in Figure 1 (Table 1).

In the course of this study, we first examined the surface adsorption of the hyperbranched molecules from a solution on a bare silicon substrate according to the procedure described earlier.[34] For the hyperbranched core **G3**, we observed the formation of a uniform adsorbed film with the ultimate thickness of 3.0 nm. These bilayered films were stabilized by a network of hydrogen bonding between surface SiOH groups and terminal hydroxyl groups of hyperbranched polymers. In contrast, epoxy-functional hyperbranched molecules of the **EHBP** compound showed weak adsorption on the bare silicon. Obviously, the hydrophobic shell of predominantly alkyl branches prevented the formation of anchored macromolecules on a hydrophilic silicon surface. Therefore, we exploited chemical grafting from melt to fabricate the **EHBP** layer by using the known reaction between silanol groups and epoxy groups initiated at elevated temperatures (Scheme 2).[35,36] The crucial point was to find a balance between the rate of grafting of epoxy-containing branches and the rate of dewetting caused by the interaction between hydrophobic branches and the hydrophilic silicon surface. We varied grafting conditions, such as concentration of the solution, thickness of the initial film, grafting time, and temperature, to avoid the dewetting phenomenon and ensure the formation of anchored and robust uniform layers. We observed that the initial thickness of about 300 nm provided for the best grafted films. Then, for temperatures below 120 °C, we observed nonuniform surface morphology with depleted areas of poorly grafted

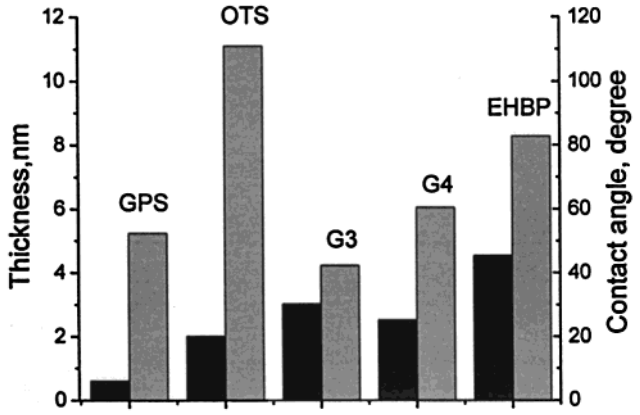

Figure 2. Comparison of contact angles (gray columns) and the thickness (black columns) of the **EHBP** layer obtained in this work with the layers of polyester cores of two different generations, **G3** and **G4** (ref 34), epoxy-terminated SAM (GPS, ref 36), and alkyl-terminated SAM (OTS, ref 7).

material. On the other hand, at temperature higher 150 °C, inhomogeneous surface morphology was revealed that reminds typical dewetting patterns. Apparently, this phenomenon was caused by high mobility of polymer melt and unfavorable interactions between predominantly hydrophobic peripheral groups and silicon oxide surface. Under these conditions, dewetting rate exceeded significantly the rate of chemical grafting that prevented the formation of uniform and dense surface layer.

As we observed, grafting from the melt within the temperature interval of 120−150 °C resulted in steady growth of the polymer films. The thickness reached the ultimate value of 4.5 nm after 1 h of grafting (Table 1). AFM images of the **EHBP** layers obtained at 120 °C for different grafting times are displayed in Figure 3. After 10 min of grafting, the incomplete layer possessed islandlike surface morphology. The increase of the grafting time resulted in gradual increase of surface coverage. The **EHBP** layer became almost uniform after 15 min of grafting (Figure 3). The surface coverage increased to 80% and the contact angle reached 60°. After 20 min of grafting, the layer demonstrated very smooth and uniform surface morphology, though the thickness reached the plateau value only after 1 h of grafting. The contact angle also reached the constant value of 82°. This value was much higher than one observed for the core **G3** (42°) and epoxy-terminated SAM studied earlier (52°) due to the presense of the hydrophobic terminal branches (Table 1). On the other hand, it was well below the contact angle observed for alkyl chains (110°),[37] which indicates substantial deviation of surface composition from one expected for surfaces fully saturated with alkyl chains.

The optimized complete **EHBP** layer was uniform with the rms microroughness about 0.2 nm as evaluated from AFM images within the 1 × 1 μm surface area (Figure 3). The thickness of the layer, measured from the depth of the through hole produced by scanning with

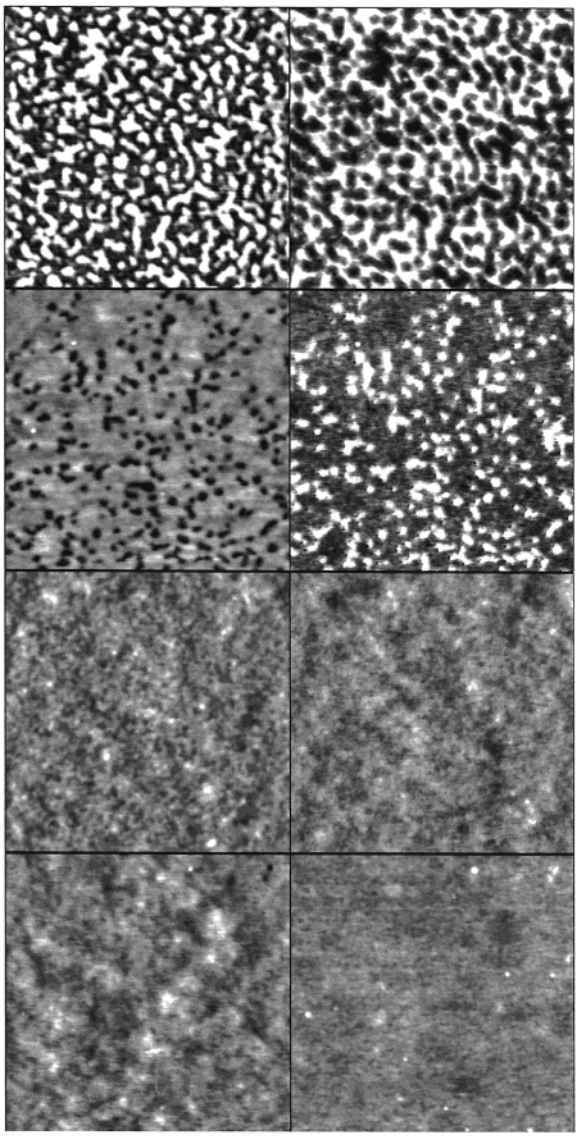

Figure 3. AFM images (topography (left) and phase (right)) of the **EHBP** layer at different stages of formation at 120 °C: 10, 15, 20, and 70 min of grafting (from top to bottom). Scan size is 1 × 1 μm, height scale is 5 nm, and phase scale is 30°.

high forces, was 4.4 ± 0.3 nm, which was in good agreement with the value obtained from ellipsometry measurements for several independently fabricated polymer films. The thickness of the layer was close to the diameter of the molecules in a globular shape (estimated to be within 3.5−4.5 nm from molecular modeling) (Table 1). To obtain further insight into chemical composition of the layers and their internal microstructure, we turn to the results of XPS measurements (Tables 2 and 3).

Observational XPS spectra showed the presence of all elements expected for the given polymer layer (Figure 4). Change of the takeoff angle from 0°, to 60°, and to 75°, which corresponded to the probing depth of 8, 4, and 2 nm, respectively, led to a significant decrease of silicon peak intensities and redistribution of oxygen and carbon peak intensities toward higher intensity of the carbon peak. The latest result reflected the decreasing oxygen content due to reducing contribution from the silicon dioxide layer as was estimated from high-resolution spectra (Figure 5). In addition, the ratio of "organic" oxygen to carbon was estimated to be 1:4 for

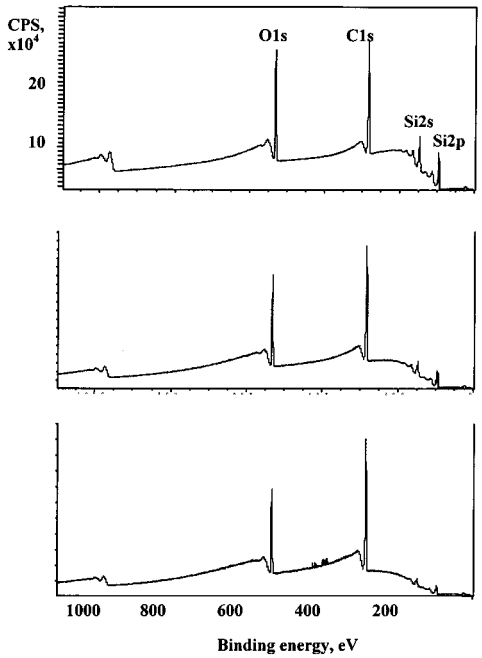

Figure 4. XPS survey spectra for the **EHBP** layer at three different takeoff angles: 0° (top), 60° (middle), and 75° (bottom) corresponding to different thicknesses analyzed (Table 3).

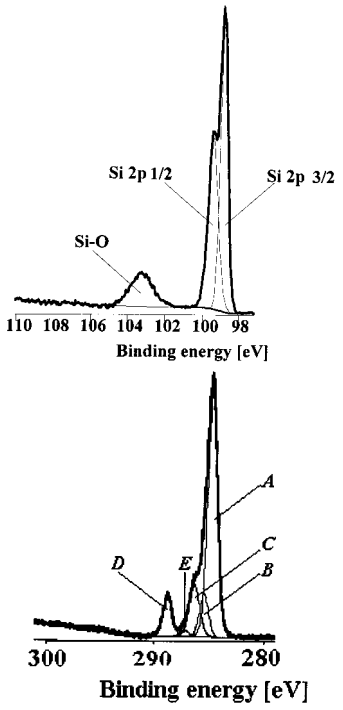

Figure 5. High-resolution XPS spectra for the **EHBP** layer for different elements: silicon (top, 0° takeoff angle) and carbon (bottom, 60° takeoff angle). Data for splitting maxima for the carbon elements (according to Scheme 3) is presented in Table 3.

the entire polymer layer that was close to the ratio estimated from the idealized chemical structure and indicated authentic chemical microstructure of the grafted layer (Table 3).

On the other hand, the reduced carbon (CH_2) content as compared to idealized chemical structure (by 11%) indicated internal imperfections of hyperbranched polymers such as branch cross-linking and termination. These internal defects reduced the number of terminal branches per the polar core from 32 (characteristic of

Table 2. XPS Characterization of the Chemical Composition of EHBP Layer

conditions	chemical composition in atomic % for different carbon atoms shown in bold (energy is in eV)				
see Scheme 3:	A **C**-H_2 (285.0)	B **C**-COO (285.8)	C **C**-O-**C** and **C**-OH (286.7)	D O-**C**=O, ester (289.2)	E **C**-O-**C**, epoxy (287.7)
probing depth, 2 nm	66.6	9.2	14.1	9.2	0.9
probing depth, 4 nm	66.2	9.4	13.7	9.4	1.3
probing depth, 8 nm	60.0	10.9	16.9	10.9	1.4
idealized chemical structure (Figure 1)	68.2	9.1	10.3	9.1	3.3

Table 3. XPS Characterization of the Element Ratio for the EHBP Layer

element ratio	complete layer	uppermost 2 nm
O: C, exptl	1:4	1:7
O: C, model estimation Figures 1 and 6	1:3.7	1:7

the idealized structure) to fewer than 29. However, the uppermost 2 nm layer showed significant enhancement with carbon element that indicated predominant surface localization of the terminal alkyl branches with more polar segments being near the silicon surface. Indeed, detailed analysis of the high-resolution spectra for carbon element confirmed this conclusion.

High-resolution C 1s spectra were decomposed into five component peaks (A, B, C, D, and E) reflecting the different chemical environment of carbon atoms (Figure 5, Table 2). These peaks were assigned to the specific chemical groups presented in the branches as shown in Scheme 3 and in accordance with the known binding energies.[38] The areas of the two component peaks B and D were close, because of their stoichometric ratio in the chemical microstructure, [B]:[D] = 1:1. Peak C was larger than either peak B or D. In addition to the ester groups (O=**C**−O−C), the polymer contained additional ether groups (**C**−O−**C**) or alcohol groups (**C**−OH), which can be partially formed by opening of the fraction of the epoxy rings. The band E found was found to be located at somewhat higher binding energy than the expected value for epoxy groups (E = 287.02 eV). This shift can be attributed to the secondary nature of the epoxy groups. Another possible candidate, the ketone group, is not in the chemical composition of the molecules. Other structure elements with similar binding energy that can contribute to this peak could be the Si−O−**C** bond, which can be formed as a result of chemical grafting. However, the expected amount of those bonds was too low to separate the corresponding component peak (**Si**−O−C) in the Si 2p spectrum (expected at BE = 102.0 eV).[38]

Analysis of the chemical composition showed fair correspondence of expected and calculated values with reduction of the aliphatic carbon component as was discussed above (Table 2). These data confirmed preferable localization of the terminal alkyl chains closer to the layer surface. The content of the core polar segments

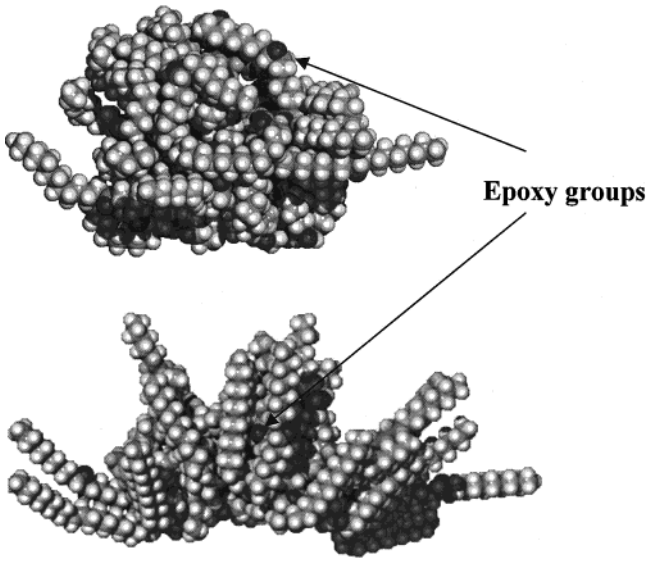

Figure 6. Molecular models of **EHBP** molecules in globular conformation (top) and in the conformation with the polar core spreading over the silicon surface and alkyl terminal chains locating close to the surface uppermost layer (bottom).

was slightly higher in the vicinity of the surface. The content of the epoxy groups was significantly (3 times) lower than theoretical value. This reduction could be explained considering partial "consumption" of the epoxy rings during grafting of the macromolecules to the silicon oxide surface. From the element composition measured, we can estimate that about 40% of epoxy groups was still present within the layer with 3−4 groups per molecule being localized within 2 nm from the surface.

These results, in conjunction with ellipsometric and AFM data discussed above, allowed proposing the "segregated" model of hyperbranched molecules as an alternative to globular, spherical conformation (Figure 6). This model reflects the predominant interaction of the polar core with a polar substrate. Redistribution of dissimilar molecular segments included preferential adsorption of the polar core on the silicon surface with a lesser fraction of the terminal branches in close proximity to the surface. Such redistribution resulted in a higher fraction of the alkyl terminal branches

Scheme 3. Fragment of HPB Branch with Designated Atomic Groups As Defined from XPS Spectra

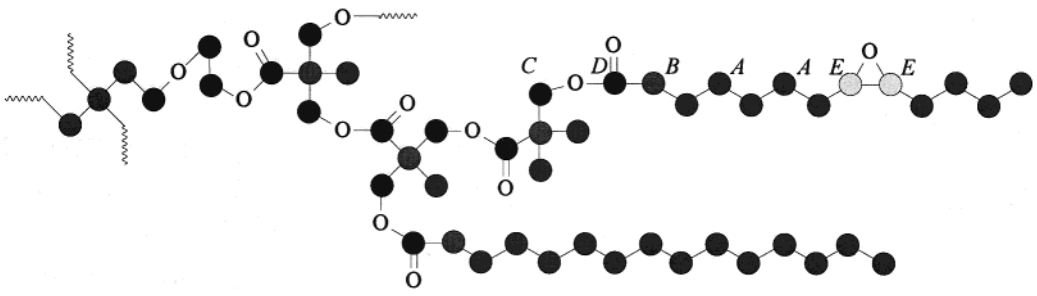

positioned closer to the film surface (Figure 6). This microstructure is based on our previous results on conformation of hyperbranched cores that demonstrated **G3** cores being squeezed on a silicon surface to a pancake shape with a height of 1.5−1.9 nm.[34] The uppermost layer of 2−3 nm should be filled with terminal alkyl branches to complain with experimentally observed thickness of 4−5 nm (Figure 6). This type of microstructure is similar to one proposed for the interfacial assemblies of dendrimers with polar cores and is considered to be common for dendrimers with compliant cores, low-generation dendrimers, and very dissimilar chemical composition of cores and shells.[39] However, it is clear that a simple representation with one of the models from Figure 6 oversimplifies the real microstructure of the functionalized hyperbranched layer. The actual structure is more complicated with gradual changes of segment/composition distribution across the layer. Significant polydispersity of hyperbranched molecules should contribute to complex layer microstructure with smaller macromolecules packed on top each other and larger macromolecules being in a more compressed state.

An independent estimation of surface properties by using contact angle values confirmed a mixed composition of the layer surface. The measured value of the contact angle for the **EHBP** layer was well below 110° expected for pure alkyl branches (Table 1). This can be attributed to the surface presence of the epoxy groups. To evaluate the fractional presence of the epoxy groups on the layer surface, we used the Cassie equation for the two-component surfaces considering epoxy groups and alkyl chains as two major components affecting the surface properties.[37] We applied the Cassie equation to the two-component surface using the contact angle values of 110° and 52° for the alkyl- and epoxy-terminated SAM surface,[40] respectively (Table 1). As a result, we obtained the estimation of a surface fraction of epoxy groups of about 40%, which is close to the XPS estimation.

Measurements of the interfacial properties of the polymer layers provided additional independent information regarding their physical state and surface functionality. To obtain independent confirmation of the presence of epoxy groups within uppermost surface layer and its ability to anchor molecules, we conducted two additional experiments. One of them was grafting from melt of a triblock copolymer, poly[styrene-*b*-(ethylene-*co*-butylene)-*b*-styrene] (SEBS), functionalized with 2% maleic anhydride (Kraton, Shell) according to the procedure described before.[41] Another experiment was performed by the treatment of the EHBP layer with *n*-butylamine from the 0.1% solution in ethanol for 24 h and subsequent multiple washing with ethanol and THF.

Recently, we have shown that the SEBS copolymer can be grafted to epoxy-terminated SAM.[41] We reproduced the conditions of SEBS grafting using the **EHBP** layer as a substrate. We found 8.5 ± 0.5 nm thickness of the SEBS formed on the **EHBP** layer, which was identical to the value obtained earlier. Moreover, the grafted SEBS layer demonstrated similar nanodomain morphology (Figure 7). This layer sustained, without damage, significant (up to 1 μN) shear stress and harsh washing procedure including a combination of hot polar solvent and ultrasonic bath. We concluded that the **EHBP** layer possessed anchoring ability similar to

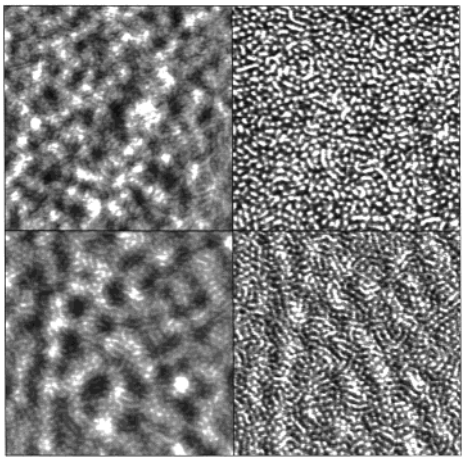

Figure 7. AFM images (topography (left) and phase (right)) of the SEBS layer grafted on the **EHBP** layer (top) and the SEBS layer grafted on epoxy-terminated SAM (bottom, after ref 37).

epoxy-terminated SAM. On the other hand, *n*-butylamine adsorbed from solution under mild conditions was completely washed out from the **EHBP** layer surface. We suggest that, in this case, both the secondary nature of epoxy groups and the hydrophobic alkyl-predominated surface were responsible for the inhibition of a surface reaction.

The **EHBP** layer grafted to a silicon surface is expected to be much more robust and mechanically stable and to sustain much higher shear stresses than physically adsorbed polymer layers. Therefore, we conducted additional experiments to verify the micromechanical properties of this layer and its shear stress resistance. AFM scanning in the contact mode of the 1 × 1 μm surface area was performed for all layers with the same probe and under the same conditions. First, we observed that the layer sustained very high shear stresses produced by the AFM tip scanning under normal load up to 1 μN, which easily damaged a physically adsorbed layer of polar hyperbranched cores **G3**. Scanning with forces higher than 1 μN could damage the grafted layer by scrapping the material within the surface area scanned as demonstrated in Figure 8. This level of the anchoring strength to the substrate is typical for chemically grafted polymer and organic layers.[41] We carried out comparative measurements of the wear stability of the grafted **EHBP** layer and epoxy-terminated SAMs. We moved the location and applied increasing normal loads to estimate the wear stability at low, moderate, and high loads. Then, the sample damage was visualized with tapping mode by zooming out the worn area (Figure 8). The reference sample of the epoxysilane SAM demonstrated increasing damage of the surface with the increasing load with debris of organic materials flying over the damaged area even at modest loads. In contrary, the grafted **EHBP** layer sustained low load of 250 nN and showed very light wear at moderate loads. Even at the highest load, about 1 μN, the vast majority of the surface area on the **EHBP** layer was kept untouched. Obviously, grafted hyperbranched polymer layer was more wear resistant than low-molar organic SAM due to its ability to reversible elastic deformation under high shear stresses.

To test these micromechanical properties, we performed micromapping of the **EHBP** layer as described elsewhere (Figure 9).[27] The matrix of 32 × 32 probing

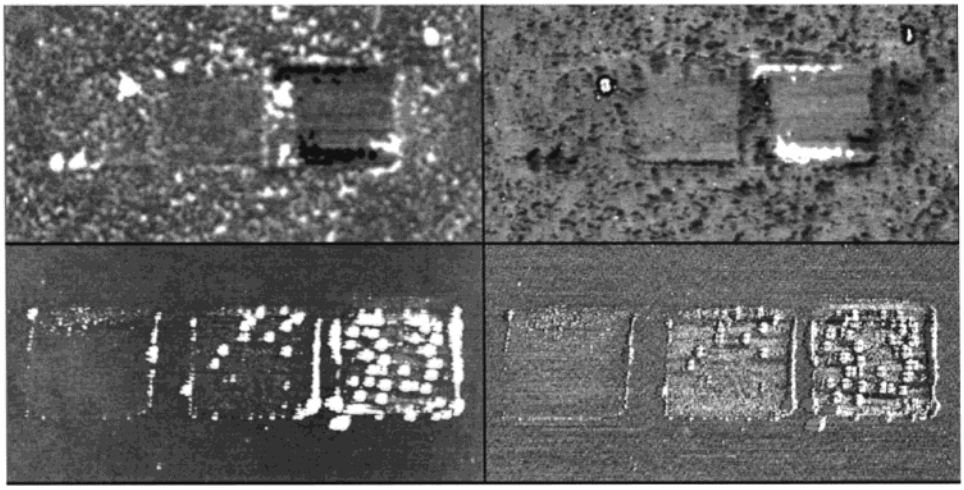

Figure 8. AFM images (4 × 2.5 μm, topography (left) and phase (right)) of the **EHBP** layer (top) and epoxy-terminated SAM (bottom) being a subject of preceding scannings within the 1 × 1 μm area with low, modest, and high (sequential tracks from left to right) forces.

pixels was used to evaluate surface distribution of compression elastic modulus and adhesive forces with lateral resolution close to 30 nm. We took precautions to ensure pure elastic deformation during multiple indentations by controlling maximum deflection and zooming out to observe appearance of indentation marks. It was observed that the **EHBP** layer indeed sustained very significant reversible deformations with compression as high as 80%. As clear from elastic and adhesive "images", the surface distribution of both properties was statistically uniform (Figure 9). Surface histograms were relatively narrow with standard deviation below 5% for adhesive forces and 25% for elastic modulus, *E*. The apparent elastic modulus of the layer was about 300 MPa due to the contribution of a stiff silicon substrate. To account this contribution, we applied the double-layer model described elsewhere.[42] This model considers cooperative deformation of two independent layers with different elastic moduli. Within the double-layer model, we obtained the value of elastic modulus for the **EHBP** layer of 11 MPa (Figure 9). This value was close to typical moduli for cross-linked rubber surfaces[27] and demonstrated superior elastic response of the grafted layer due to the presence of both internal cross-linkings and multiple grafting to the solid surface. This is in striking contrast with viscous fluid state of **EHBP** molecules in the bulk state.

Conclusions

In conclusion, we demonstrated that robust and uniform monolayers with the thickness of 4.5 nm could be fabricated by the chemical grafting of functionalized hyperbranched polyesters from melt to a bare silicon surface. The multifunctionality of the peripheral chains (epoxy-alkyl) provided dual ability for both grafting to solid substrate and hydrophobization of the surface. Steric constraints imposed by the chemical attachment of both terminal alkyl and epoxy-alkyl chains prevented microphase separation within ultrathin polymer layer. An estimated 3−4 epoxy groups per molecule were located in the uppermost surface layer and provided surface functionality sufficient to graft another polymer layer with appropriate functionality. Grafted hyperbranched polymer layers were elastic and robust due to both internal cross-linking and grafting to the solid surface. They sustained high compression and shear

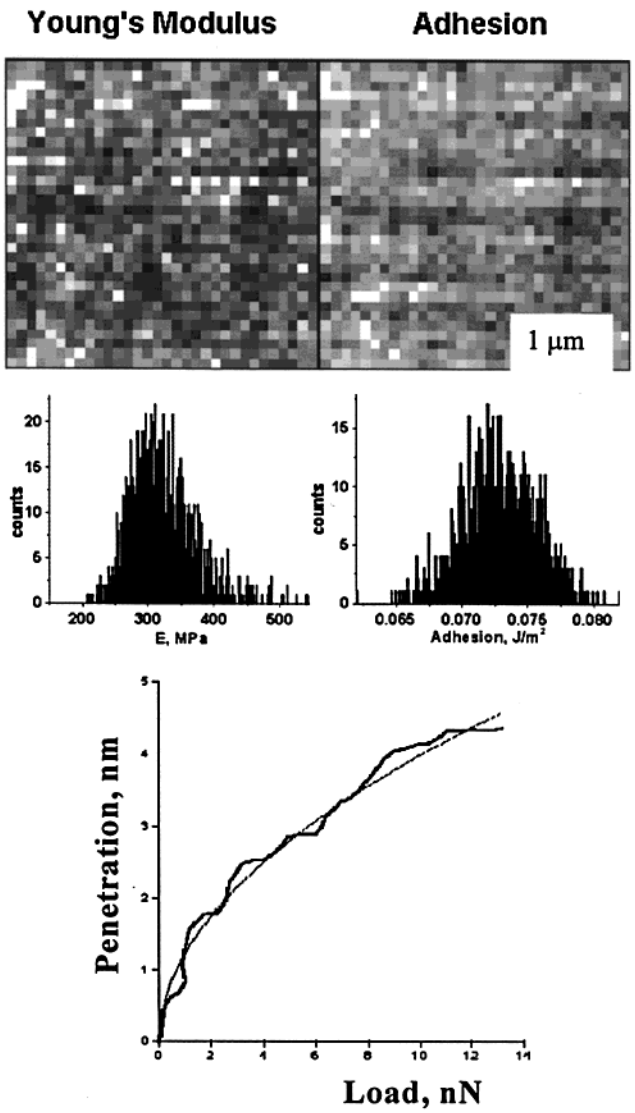

Figure 9. Surface distribution of the elastic modulus and adhesive forces for the **EHBP** layer obtained with 32 × 32 sequential probings within the 1 × 1 μm surface area (top); corresponding histograms of surface distribution of elastic and adhesive properties (middle); an example of experimental data for layer deformation vs normal load (bold solid line) along with double-model theoretical fit (solid line).

stresses much higher than low-molar organic SAMs and conventional polymer brushes anchored via one end group.

Acknowledgment. Funding was from the National Science Foundation, Grants CMS-0099868 and DMR-0074241. The authors are grateful to P. D. Bloom and V. Sheares for GPC analysis and to A. Greco, S. Minko, and S. Peleshanko for useful discussions and technical assistance. The authors also thank Perstorp Polyols Inc. and personally Jeffrey Jones (Perstorp Polyols, Toledo, OH) and Birger Midelf (Perstorp Specialty Chemicals AB, Sweden) for sample donation and very useful technical discussions.

References and Notes

(1) Ulman, A. *Introduction to Ultrathin Organic Films*; Academic Press: San Diego, 1991. Xia, Y.; Whitesides, G. M. *Angew. Chem.* **1998**, *37*, 550. Wilbur, J. L.; Biebuyck, H. A.; MacDonald, J. C.; Whitesides, G. M. *Langmuir* **1995**, *11*, 825.

(2) Noy, A.; Vezenov, D. V.; Lieber, C. M. *Annu. Rev. Mater. Sci.* **1997**, *27*, 381. Tsukruk, V. V.; Bliznyuk, V. N. *Langmuir* **1998**, *14*, 446. Sheller, N. B.; Petrash, S.; Foster, M. D.; Tsukruk, V. V. *Langmuir* **1998**, *14*, 4535.

(3) Sukenik, C. N.; Balachander, N.; Culp, L. A.; Lewandowska, K.; Merritt, K. *J. Biomed. Res.* **1990**, *24*, 1307. Spencer; Harder, P.; Grunze, M. *J. Am. Chem. Soc.* **1999**, *121*, 10134.

(4) Barness, Y.; Gershevitz, O.; Sekar, M.; Sukenik, C. N. *Langmuir* **2000**, *16*, 247. Beake, B. D.; Leggett, G. J. *Langmuir* **2000**, *16*, 735.

(5) Nelles, G.; Schönherr, H.; Vancso, G. J.; Butt, H.-J. *Appl. Phys. A: Mater. Sci. Process.* **1998**, *66*, 1261. Van Der Vegte, E. W.; Hadziioannou, G. *Langmuir* **1997**, *13*, 3, 4357. Xiao, X.; Hu, J.; Charych, D. H.; Salmeron, M. *Langmuir* **1996**, *12*, 235.

(6) Green, J. B.; McDermott, M. T.; Porter, M. D.; Siperko, L. M. *J. Phys. Chem.* **1995**, *99*, 10960. McDermott, M. T.; Green, J. B.; Porter, M. D. *Langmuir* **1997**, *13*, 2504. Marti, A.; Hähner, G.; Spencer, N. D. *Langmuir* **1995**, *11*, 4632. Tsukruk, V. V. *Adv. Mater.* **2001**, *13*, 95.

(7) Tsukruk, V. V.; Bliznyuk, V. N.; Hazel, J.; Visser, D.; Everson, M. P. *Langmuir* **1996**, *12*, 4840.

(8) Halperin, A.; Tirrell, M.; Lodge, T. P. *Adv. Polym. Sci.* **1992**, *100*, 33. Milner, S. T. *Science* **1991**, *251*, 905.

(9) Zhao, B.; Brittain, W. J. *Prog. Polym. Sci.* **2000**, *25*, 677. Sidorenko, A.; Minko, S.; Schenk-Meuser, K.; Duschner, H.; Stamm, M. *Langmuir* **1999**, *15*, 8349.

(10) Foster, M. D.; Sikka, M.; Singh, N.; Bates, F. C.; Satija, S. K.; Majkrzak, C. F. *J. Chem. Phys.* **1992**, *96*, 8605. Lee, L. H. *Adhesion and Adsorption of Polymers*; Plenum Press: New York, 1980. Luzinov, I.; Minko, S.; Senkovsky, V.; Voronov, A.; Hild, S.; Marti, O.; Wilke, W. *Macromolecules* **1998**, *31*, 3945.

(11) Karim, A.; Tsukruk, V. V.; Douglas, J. F.; Satija, S. K.; Fetters, L. J.; Reneker, D. H.; Foster, M. D. *J. Phys. II* **1995**, *5*, 1441. Luzinov, I.; Julthongpiput, D.; Malz, H.; Pionteck, J.; Tsukruk, V. V. *Macromolecules* **2000** *33*, 1043.

(12) Zhulina, E. B.; Wolterink, J. K.; Borisov, O. V. *Macromolecules* **2000**, *33*, 4945.

(13) Kim, Y. H.; Webster, O. W. *J. Am. Chem. Soc.* **1990**, *112*, 4592. Hawker, C. J.; Lee, R.; Frechet, J. M. J. *J. Am. Chem. Soc.* **1991**, *113*, 4583. Voit, B. *J. Polym. Sci., Part A* **2000**, *38*, 2505. Hult, A.; Johansson, M.; Malmstrom, E. *Adv. Polym. Sci.* **1999**, *143*, 1. Ihre, H.; Johansson, M.; Malmstrom, E.; Hult, A. *Adv. Dendritic Macromol.* **1996**, *3*, 1. Voit, B. *J. Polym. Sci., Part A* **2000**, *38*, 2505.

(14) Tsukruk, V. V. *Adv. Mater.* **1998**, *10*, 253. Sheiko, S.; Moller, M. *Top. Curr. Chem.* **2001**, *212*, 137. Tully, D. C.; Frechet, M. J. *Chem. Commun.* **2001**, 1229.

(15) Bruening, M. L.; Zhou, Y.; Aguilar, G.; Agee, R.; Bergbreiter, D. E.; Crooks, R. M. *Langmuir* **1997**, *13*, 770. Hierlemann, A.; Campbell, J. K.; Baker, L. A.; Crooks, R. M.; Ricco, A. J. *J. Am. Chem. Soc.* **1998**, *120*, 5323. Wells, M.; Crooks, R. M. *J. Am. Chem. Soc.* **1996**, *118*, 3988.

(16) Mezzenga, R.; Boogh, L.; Manson, J.-A. E.; Pettersson, B. *Macromolecules* **2000**, *33*, 4373.

(17) Soerensen, K.; Pettersson, B. In *PCT Int. Appl.*; 9612754: WO, 1996**.** Pettersson, B. In *PCT Int. Appl.*; 9723538: WO, 1997**.**

(18) Mock, A.; Burgath, A.; Hanselmann, R.; Frey, H. *Macromolecules* **2001**, *34*, 7692. Gong, C.; Miravet, J.; Frechet, J. M. *J. Polym. Sci., Part A* **1999**, *37*, 3192.

(19) Emrick, T.; Chang, H.; Frechet, J. M. *Macromolecules* **1999**, *32*, 6380. Gong, C.; Frechet, J. M. *Macromolecules* **2000**, *33*, 4997. Gong, C.; Frechet, J. M. *J. Polym. Sci., Part A* **2000**, *38*, 2970.

(20) Boogh, L.; Pettersson, B.; Manson, J. A. *Polymer* **1999**, *40*, 2249. Ratna, D.; Simon, G. P. *Polymer* **2001**, *42*, 8833. Oh, J.; Jang, J.; Lee, S. *Polymer* **2001**, *42*, 8339. Mezzenga, R.; Plummer, C. J.; Boogh, L.; Manson, J. A. *Polymer* **2001**, *42*, 305.

(21) Emrick, T.; Chang, H.; Frechet, J. M.; Woods, J.; Baccei, L. *Polym. Bull. (Berlin)* **2000**, *45*, 1.

(22) Azzam, R. M. A.; Bashara, N. M. *Ellipsometry and Polarized Light*; North-Holland Pub. Co.: Amsterdam, 1977.

(23) Aranishi, Y.; Takahashi, H. *Jpn. Kokai Tokkyo Koho* **2000**, 6. JKXXAF JP 2000226727 A2 20000815.

(24) Van Krevelen, D. W. *Properties of Polymers*; Elsevier: Amsterdam, 1997.

(25) Tsukruk, V. V.; Reneker, D. H. *Polymer* **1995**, *36*, 1791. Tsukruk, V. V. *Rubber Chem. Technol.* **1997**, *70*, 430. Ratner, B., Tsukruk, V. V., Eds.; *Scanning Probe Microscopy of Polymers*; *ACS Symp. Ser.* **1998**, 694.

(26) Chizhik, S. A.; Ahn, H.-S. *Appl. Phys. Lett.*, in press.

(27) Tsukruk, V. V.; Gorbunov, V. V. *Probe Microsc.*, in press. Chizhik, S. A.; Huang, Z.; Gorbunov, V. V.; Myshkin, N. K.; Tsukruk, V. V. *Langmuir* **1998**, *14*, 2606.

(28) Tsukruk, V. V.; Huang, Z. *Polymer* **2000**, *41*, 5541.

(29) Cleveland, J.; Manne, S.; Bocek, D.; Hansma, P. K. *Rev. Sci. Instrum.* **1993**, *64*, 403.

(30) Hazel, J. L.; Tsukruk, V. V. *Thin Solid Films* **1999**, *339*, 249. Hazel, J.; Tsukruk, V. V. *J. Tribology* **1998**, *120*, 814.

(31) Vesenka, J.; Manne, S.; Giberson, R.; Marsh, T.; Henderson, E. *Biophys. J.* **1993**, *65*, 992.

(32) Simon, F.; Jacobasch, H. J.; Spange, S. *Colloid Polym. Sci.* **1998**, *276*, 930.

(33) Cerius^2 3.9; Molecular Simulations Inc.: San Diego, 1997.

(34) Sidorenko, A.; Zhai, X. W.; Peleshanko, S.; Greco, A.; Shevchenko, V. V.; Tsukruk, V. V. *Langmuir* **2001**, *17*, 5924.

(35) Kalal, J.; Tlustakova, M. *Acta Polym.* **1979**, *30*, 40.

(36) Xue, G.; Ishida, H.; Koenig, J. E. *Angew. Makromol. Chem.* **1986**, *140*, 127. Heublein, G.; Heublein, B.; Hortchansky, P.; Meissner, H.; Schultz, H. *J. Macromol. Sci.* **1988**, *A25*, 183.

(37) Adamson, A. W. *Physical Chemistry of Surfaces*; John Wiley & Sons: New York, 1990.

(38) Spange, S.; Muller, H.; Pleul, D.; Simon, F. *Stud. Surf. Sci. Catal.* **2001**, *132*, 301. Ameen, A. P.; Ward, R. J.; Short, R. D.; Beamson, G.; Briggs, D. *Polymer* **1993**, *34*, 1795. Beamson, G.; Briggs, D. *High-Resolution XPS of Organic Polymers*; John Wiley: Chichester, UK, 1992.

(39) Zhang, X.; Wilhelm, M.; Klein, J.; Pfaadt, M.; Meijer, E. W. *Langmuir* **2000**, *16*, 3884. Sayed-Sweet, Y.; Hedstrand, D. M.; Spinder, R.; Tomalia, D. *J. Mater. Chem.* **1997**, *7*, 1199.

(40) Luzinov, I.; Julthongpiput, D.; Liebmann-Vinson, A.; Cregger, T.; Foster, M. D.; Tsukruk, V. V. *Langmuir* **2000**, *16*, 504. Tsukruk, V. V.; Luzinov, I.; Julthongpiput, D. *Langmuir* **1999**, *15*, 3029.

(41) Luzinov, I.; Julthongpiput, D.; Tsukruk, V. V. *Macromolecules* **2000**, *33*, 7629.

(42) Chizhik, S. A.; Gorbunov, V. V.; Fuchigami, N.; Luzinov, I.; Tsukruk, V. V. *Macromol. Symp.* **2001**, *167*, 169.

MA011682T